*Review Article*

# A comprehensive review of the common developmental disorders of hip – Developmental dysplasia of the hip, slipped capital femoral epiphysis, and Perthes disease

Pavithra Subramanian[1,#], Raghuraman Soundararajan[1,#], Stanzin Spalkit[2], Anindita Sinha[3], Nikita Verma[3]

[1]Department of Radiodiagnosis, All India Institute of Medical Sciences, Nagpur, Maharashtra, [2]Department of Radiodiagnosis and Interventional Radiology, All India Institute of Medical Sciences, New Delhi, [3]Department of Radiodiagnosis, Post Graduate Institute of Medical Education and Research, Chandigarh, India.

[#]Pavithra Subramanian and Raghuraman Soundararajan have contributed equally and share first authorship.

**\*Corresponding author:**
Raghuraman Soundararajan,
Assistant Professor,
Department of Radiodiagnosis,
All India Institute of Medical
Sciences, Nagpur, Maharashtra,
India

raghuraman.raju93@gmail.com

## ABSTRACT

Developmental disorders of the hip joint are common in pediatric and adolescent populations, and imaging plays a pivotal role in their diagnosis and follow-up. Timely diagnosis and appropriate management are crucial to prevent complications, which can lead to long-term morbidity and poor quality of life. This article outlines the relevant aspects of normal hip development and reviews the imaging considerations in the common developmental hip disorders – developmental dysplasia of the hip (DDH), Legg–Calve–Perthes disease (LCPD), and slipped capital femoral epiphysis (SCFE). DDH results from acetabular or femoral head dysplasia and affects neonates, infants, and toddlers. Ultrasonography is the workhorse of diagnosis in neonates and infants before epiphyseal ossification. Radiographs are used for diagnosis in toddlers and older children, while magnetic resonance imaging (MRI) plays a significant role in cases with diagnostic dilemma. LCPD affects young boys in the age group of 2–14 years and is characterized by idiopathic osteonecrosis of the femoral head. Radiographs and MRI play the major role in the diagnosis and staging of LCPD. Depending on the stage of disease, radiographs show epiphyseal flattening, fragmentation, metaphyseal hyperlucency, etc., on radiographs and there may be corresponding altered epiphyseal T1 signal intensity, with subchondral T2 hyperintensity and femoral head deformation on MRI. SCFE is a type I Salter Harris injury with epiphyseal slip, affecting adolescents (predominantly males). Radiographs and MRI are primarily used for diagnosis and reveal epiphyseal slip with physeal edema and joint effusion/synovitis. Timely identification and management of SCFE avoids complications such as avascular necrosis, femoroacetabular impingement, and secondary osteoarthritis.

**Keywords:** Developmental dysplasia, Hip joint, Legg–Calve–Perthes disease, Slipped capital femoral epiphysis

## INTRODUCTION

The hip joint development is a complex process which occurs under the influence of genetic and hormonal factors. It starts *in utero* and continues until adulthood. Deviation from normal developmental processes results in developmental disorders of the hip, which can present in any age group, ranging from neonate to adolescents. This article is limited to the three common developmental hip disorders, that is, developmental dysplasia of the hip (DDH), Legg–Calve–Perthes disease (LCPD), and slipped capital femoral epiphysis (SCFE). DDH is common in neonates, infants, and toddlers and presents as limb length discrepancy, asymmetric gait or hip pain, depending on the patient's age. LCPD affects children between 2 and 14 years of age, with peak incidence at 5–6 years of age, with a predilection for boys. The clinical presentation

is with unilateral hip pain and a limp. SCFE is typically seen in obese adolescent males, commonly affecting those in the age group of 12–15 years. Depending on the degree of epiphyseal slip, patients may have mild to severe hip pain, sometimes restricting them from walking. Thus, in a pediatric patient presenting with unilateral hip pain, these three developmental disorders need to be considered as differential diagnoses. While some of the differentials can be excluded based on the age of presentation and associated history, imaging plays a pivotal role in arriving at the correct diagnosis and guiding the management. In a neonate/infant with limb length discrepancy, ultrasonography (US) is the workhorse, to rule out DDH, which is the most common hip disorder in this population. Radiographs of the pelvis with both hips (frontal and frog leg views) are the primary imaging modality in older children presenting with hip pain. DDH, LCPD, and SCFE (after the slip) are well-visualized on radiographs. Magnetic resonance imaging (MRI) plays an important role in cases with diagnostic dilemma and to evaluate complications. Computed tomography (CT) is generally not preferred due to ionizing radiation, which, however, can be used for three-dimensional visualization of the hip joint, particularly for surgical planning and post-operative evaluation.

## DEVELOPMENT OF A NORMAL HIP

The prenatal and antenatal development of the hip joint follows a genetically orchestrated sequence directed by cell signaling factors. Knowledge of the journey of hip development is essential to understanding the aberrations in the process and the resultant disorders. By the 8th week post-fertilization, joint differentiation is completed. The acetabulum is initially formed by the differentiation of precursor cells of the ilium, ischium, and pubis (in that sequence).[1] It develops as a depression proximal to the femur, starting from 6 weeks post-fertilization. The differentiation of acetabulum, particularly the ilium, lags behind that of the femoral head, leading to a physiological under-coverage of the femoral head.

The acetabular cartilage complex at birth consists of the acetabular cartilage laterally and the triradiate cartilage medially. These later form the acetabular rim and the non-articular medial acetabular wall, respectively. The acetabular height and width depend on the interstitial growth of the triradiate cartilage. It is pertinent to note that the final acetabular shape is, however, strongly dependent on its interaction with a spherical femur head.[2,3]

## DDH

DDH, as the name suggests, occurs due to an abnormal development of the hip. It comprises a spectrum of aberrations, including hip instability, acetabular dysplasia, hip subluxation, and dislocation. Since all these manifestations may not be present at birth, the older term "congenital dysplasia of the hip" is no longer used. The incidence of DDH is around 1 in 1000 births, with a predilection for females due to ligamentous laxity from maternal hormonal influence.[4] It is unilateral in 63% of cases, with the left hip being more commonly affected.[5]

### Risk factors and etiopathogenesis

The normal development of the acetabulum and femoral head are interdependent and are based on a genetically determined balance. The aberrations in growth affect all structures in the hip joint, including the acetabulum, proximal femur, and soft components. The excessive pressure exerted on the labrum by a dislocated or subluxated femoral head promotes fibrocartilage hypertrophy and the formation of fibrous tissue. A labral inversion may also be present in dislocated hips, which makes reduction difficult.[6] Changes in the proximal femur include shortening of the neck and delayed secondary ossification.[7]

DDH results from an interplay of hormonal, mechanical, and genetic factors. Common risk factors implicated in DDH include high progesterone levels, fetal packaging deformity (resulting from uterine abnormality/macrosomia), breech presentation, swaddling, and familial history of DDH.[6] Some chromosomal loci associated with DDH include *CX3CR*1, *GDF*5, and *HOX*.[8-10]

### Clinical presentation

Clinical features of DDH depend on the age of the child and the degree of affectation. Neonates and infants are often asymptomatic. Subtle clinical signs such as asymmetrical skin folds, discrepancy of limb lengths, and shortening of the affected thigh with hips and knees flexed (Galeazzi sign) evoke the suspicion of DDH.[11] The Barlow and Ortolani tests are standard maneuvers to clinically diagnose hip instability in neonates.[12] Limited abduction of the affected hip is also an essential pointer in infants. Clinical features in toddlers and adolescents include asymmetric gait, hip pain, and early osteoarthritis.

### Imaging in DDH

The imaging modality to diagnose DDH is decided based on the patient's age. In the first 4–6 months, when the femoral head and acetabulum are unossified, ultrasonography is the preferred imaging modality to visualize these structures and the surrounding soft-tissue landmarks. It also has the advantage of being a dynamic modality. After 4–6 months of age, the femoral head and acetabulum are ossified, obscuring the sonographic landmarks. In this population, radiography

is the standard tool to diagnose DDH.[13,14] In this age group, the ossified structures are well-visualized on radiographs.

The American Academy of Pediatrics clinical practice guidelines recommend a hip ultrasound (US) at 6 weeks of age or a hip radiograph at 4 months in girls with a positive family history of DDH or breech presentation in the third trimester.[5] According to the consensus guidelines of the Indian Academy of Pediatrics, hip ultrasound is recommended at 6 weeks of age in infants with positive Barlow test but negative Ortolani test. In infants with risk factors but normal clinical examination, further evaluation should include an ultrasound done no earlier than 6 weeks of age for infants younger than 14 weeks, ultrasound or X-ray for infants 14 weeks to 6 months of age, and X-ray for infants older than 6 months.[15,16]

MRI provides better soft-tissue visualization and is used in difficult cases and surgical planning. CT is primarily used in the post-operative period to assess procedural success.[13]

## Ultrasonography

The Graf classification of DDH is based on the morphology of the acetabulum, including the acetabular labrum, and the position and coverage of the femoral head. A high-frequency (5- or 7.5-MHz) linear array transducer is essential for performing hip ultrasonography. Sector probes distort images and should not be used in hip ultrasonography. The American Institute of Ultrasound in Medicine recommends that a standard hip ultrasound examination be performed in two orthogonal planes: A coronal view in the standard plane in a neutral position and a transverse view of the flexed hip with and without stress.[17] Three structures need to be identified on a standard ultrasound image – the vertical limb of the iliac bone (ilial line), the triradiate cartilage, and the labrum. The femoral head is also visualized on a standard plane [Figure 1]. The Graf alpha (α) and beta (β) angles are calculated based on these structures. While many machines have in-built software for measuring hip angles, these can also be measured manually. The imaging plane should be carefully selected to prevent miscalculation of Graf's angles.

The Graf α angle is the angle between the acetabular roof and the ilial line. It denotes the depth of the acetabulum, with an angle >60° indicating a normal hip with >50% acetabular roof coverage. Hence, α angle <60° is abnormal. The Graf β angle is formed between the ilial line and a line through the cartilaginous acetabular labrum. With a superolateral displacement of the femoral head, the acetabulum is elevated, with a resultant increase in β angle; a β angle >55° is abnormal. Figures 2 and 3 denote the Graf angles in a normal and dysplastic hip, respectively.
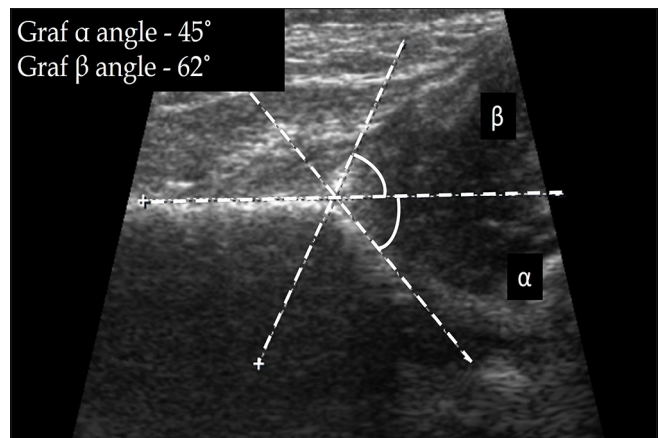
The modified Graf classification scale is based on the α and β angles [Table 1]. Types I and II depict centered hips and are differentiated based on the Graf angles. The α angle is not
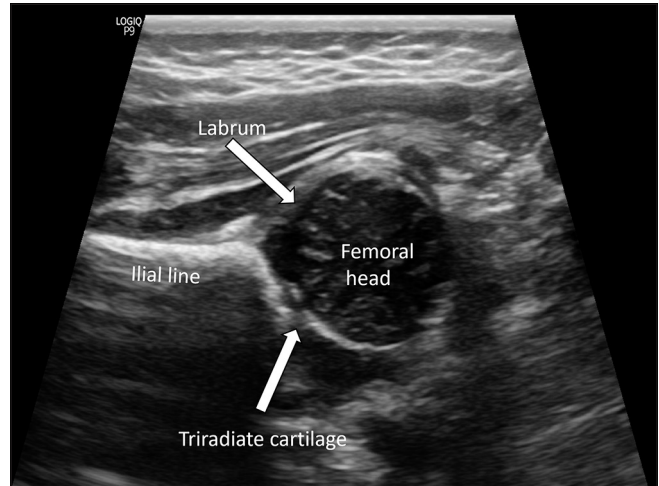


**Figure 1:** Structures of a normal hip on ultrasonography (standard plane)-the ilial line is identified as a parallel echogenic structure, representing the vertical limb of iliac bone; the unossified femoral head is seen inferior to it. The acetabular labrum and triradiate cartilage are marked by block arrows.
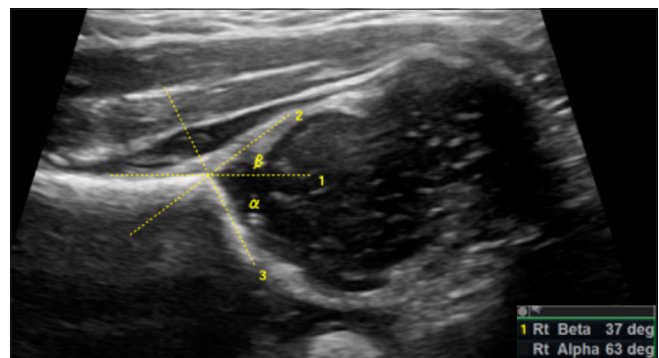


**Figure 2:** Graf alpha (α) and beta (β) angles in a normal hip-the alpha angle is between the ilial line (1) and the acetabular roof (3) and normally measures >60°. The beta angle is between the ilial line (1) and a line through the acetabular labrum (2) and normally measures <55°.



**Figure 3:** Graf angles in a case of developmental dysplasia of the hip (Graf type II c hip).

**Table 1:** Modified Graf classification scale for developmental dysplasia of hip.

| Graf type | Description | α and β angles |
|-----------|-------------|----------------|
| Type I | Normal, mature hip with >50% acetabular coverage | α >60°, β<55° |
| Type IIa | Immature, age <3 months | α=50–59° |
| Type IIb | Immature, age >3 months | α=50–59° |
| Type IIc | Deficient bony acetabulum, with concentric, but unstable femoral head | α=43–49°, β<77° |
| Type IId | Grossly subluxed femoral head, with everted labrum | α angle difficult to measure; β>77° |
| Type III | Dislocated femoral head with shallow acetabulum | |
| Type IV | Dislocated femoral head with dysplastic acetabulum and inverted labrum | |

measured in a decentered hip, and types III and IV hips are differentiated based on the acetabulum, cartilage roof, and perichondrium.[18]

**Radiography**

Anteroposterior and frog-leg lateral views of the pelvis (including both hips) are recommended to assess the hip joint.[14] A few lines and angles are described on radiographs to guide the assessment of femoral head location in relation to the acetabulum.

The *Hilgenreiner's line* is a horizontal line drawn through the right and left triradiate cartilages. The femoral head ossification center is normally superior to this. The *Perkin's line* is a line perpendicular to the Hilgenreiner's line, crossing it through the lateral margin of the acetabulum. In a normal hip, the femoral head ossification center is seen in the inferomedial quadrant, whereas in a dislocated hip, it is seen in the superolateral quadrant [Figure 4]. The *acetabular index* is an angle formed by the Hilgenreiner's line and a line extending from the lateral end of the triradiate cartilage to the lateral point of the acetabulum. It is normally <25° and is increased in hip dysplasia/dislocation [Figure 5]. The Shenton's line is an imaginary arc along the inferior border of the femur neck and the superior margin of the obturator foramen, which is normally continuous. In dysplasia, there is the inclination of the acetabulum with a centralized ossification center and an intact Shenton's line. In subluxation, the ossification center is subluxated, with a broken Shenton's line. In dislocation, the ossification center lies outside the acetabulum.[19] The central edge angle of Wiberg is an angle formed by Perkin's line and a line from the center of the femoral head to the lateral edge of the acetabulum [Figure 6]. An angle <20° is considered abnormal.



**Figure 4:** Anteroposterior (AP) radiograph of pelvis with both hips in a child with the right-sided developmental dysplasia of hip, showing Hilgenreiner's and Perkin's lines. The normal femoral head (left side) is seen in the inferomedial quadrant whereas the affected femoral head (right side) is dislocated and seen in the superolateral quadrant.



**Figure 5:** Anteroposterior (AP) radiograph of pelvis with both hips in a child with developmental dysplasia of the right hip. The acetabular index is increased on the right side (30°), whereas it is normal on the left side (15°).

**CT**

Low-dose CT is reserved as a problem-solving tool in cases with diagnostic dilemma. Postoperatively, CT can be used to assess the reduction of femoral head and in patients with surgical hardware.[13] Although CT is an excellent modality for three-dimensional visualization of anatomy, its routine usage is limited by radiation concerns in the pediatric population.

**Figure 6:** Anteroposterior (AP) radiograph of pelvis with both hips in a child with developmental dysplasia of the right hip shows measurement of central edge angle of Wieberg, which is normal on the left side. However, the lines could not be drawn on the affected side due to dislocation.

## MRI

Similar to CT, MRI is also reserved for difficult cases; however, it scores over CT due to a lack of ionizing radiation and excellent soft-tissue delineation. Acetabular morphology, retroversion, and degree of femoral head coverage can be confidently evaluated on MRI. Associated cartilaginous defects and delamination can also be looked for. Bony and cartilaginous acetabular indices can be measured, similar to radiographs. Ligamentous and soft-tissue abnormalities, such as pulvinar hypertrophy, labral eversion/inversion/hypertrophy, and ligamentum teres hypertrophy, should be ruled out, as these may hinder successful surgical reduction.[13]

## Management

Treatment of DDH is most effective in cases that are diagnosed early. Patients younger than 6 months, with reducible hip, are conservatively treated with Pavlik harnesses. In 6–18-month-old patients and those with failed Pavlik harness, closed reduction and spica casting are done. Open reduction with spica casting is reserved for patients more than 18 months of age, with failure of closed reduction. Femoral and pelvic osteotomy are performed in >2-year-old patients with severe/residual hip dysplasia.[20] Avascular necrosis (AVN) of the femoral head is the most serious complication and may result from an excessive abduction, forced closed reduction, or unsuccessful reduction.

## Summary

Thus, ultrasonography and radiographs are the primary imaging modalities in the diagnosis of DDH, depending on the status of ossification. CT and MRI play a supportive role in cases with diagnostic dilemma. MRI is particularly useful in delineating soft-tissue abnormalities, which may preclude successful surgical correction. Timely management, according to the child's age and severity of dysplasia, prevents complications. Imaging modalities used to assess the success of reduction include radiographs, CT, and MRI.

## LCPD

LCPD, also known as Perthes disease, is a common cause of painful limp occurring in 0.005–0.016% of children.[21] It represents idiopathic osteonecrosis or osteochondrosis of the femoral head, affecting children between 2 and 14 years of age, with a peak incidence between 5 and 6 years. Boys are affected more commonly than girls, with a ratio of approximately 5:1.[21,22]

### Risk factors and etiopathogenesis

The exact etiology of the disease is unknown, and the femoral head undergoes necrosis of varying degrees, which is usually self-limiting or leading to bone loss, fragmentation, or collapse of the femoral head. Thus, LCPD presents as a spectrum of mild disease to gross deformities and early osteoarthritis of the hip. Children, when diagnosed at an earlier age, tend to have a benign course and, when diagnosed later, have poorer outcomes with increased interventions.[21]

### Clinical presentation

Most cases are unilateral, and 15% of children have bilateral disease with asynchronous involvement. LCPD is a diagnosis of exclusion; secondary AVN (as a result of disorders such as sickle cell disease, steroid use, Gaucher's disease, and leukemia) and epiphyseal dysplasia should be ruled out. Children usually present with pain and limp, which may often be associated with trivial trauma or sustained activity.[23] On examination, internal rotation and abduction deficits are seen with Trendelenberg gait in the late stages.[22]

### Imaging in LCPD

#### Radiography

Plain radiographs are the initial modality of choice to assess the disease severity, extent of involvement of the femoral head, and containment of the head in the acetabular cavity. The radiographic signs depend on the severity of necrosis and the time elapsed since onset. Accordingly, the disease can be classified into three phases: The avascular/necrotic stage, the revascularization stage, and the reparative/healing stage. The imaging patterns are indicative of the disease's stage.

The early radiographic signs include joint space widening due to effusion, asymmetrically small femoral epiphysis

with an apparent increase in density, blurred physeal plate, and abnormally lucent metaphysis [Figure 7]. As the disease progresses, radiographs show flattened epiphysis, fragmentation of head, crescent sign, sagging rope sign (concave sclerotic metaphyseal line), [Figure 8] Gage sign (clear lateral image), coxa magna, and coxa vara deformity.

Five "At-risk" radiographic signs are described as signs of poor prognosis: The presence of the Gage sign, horizontal conjugal plate, lateral subluxation of the femoral head, metaphyseal reaction, and calcifications lateral to the epiphysis.

Multiple classification systems have been proposed for the disease prognostication.[22] The prognosis of LCPD is mainly based on the congruity of the femoral head, which reflects the

risk of osteoarthritis at a later age. The Stulberg classification of Perthes disease is based on this congruity and reflects the long-term risk of osteoarthritis, increasing from Stage III to V [Table 2]. It is crucial to note that the Stulberg classification should be applied only after skeletal maturity to assess residual/persistent deformity. A spherical head carries a good prognosis, whereas loss of sphericity carries a poor prognosis.[22]

The Salter-Thompson classification is based on the extent of the subchondral fracture; however, it has doubtful clinical significance. The modified Elizabethtown classification[24] is useful in staging Perthes disease and is described in Table 3.

The modified Catterall classification is an important prognostic indicator based on the degree of necrosis of the femoral head [Table 4].[22,25] Grade I disease has a good



**Figure 7:** Plain radiograph of the pelvis with both hips showing early signs of Perthes disease in the form of subtle joint space widening, mild reduction in epiphyseal height, and increased density of epiphysis on the left side (black arrow).
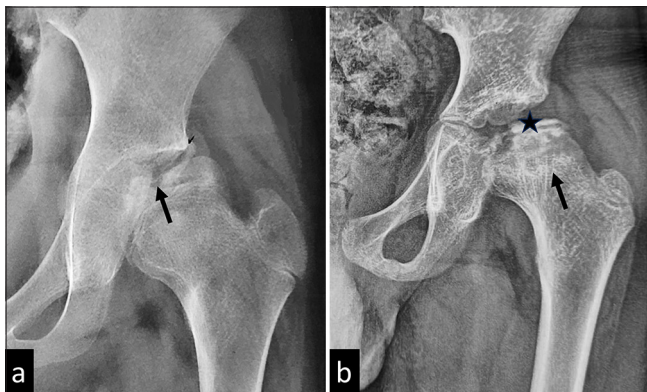


**Figure 8:** (a) Plain radiograph of a child with Perthes disease showing fragmentation of the femoral epiphysis (black arrow). (b) Plain radiograph of another child with advanced Perthes disease showing complete collapse of the femoral epiphysis (black star) and a concave metaphyseal sclerotic line (black arrow).

| Table 2: Stulberg classification of LCPD. | | |
|---|---|---|
| **Stage** | **Congruency** | **Radiographic findings** |
| I | Spherical congruency present. | Normal |
| II | Spherical congruency present, Loss of head shape is <2 mm | Spherical head with coxa magna, short neck of femur, oblique acetabulum |
| III | Aspherical congruency seen, Loss of head shape is more than 2 mm | Aspherical head, however not flattened |
| IV | Aspherical congruency seen | Flattened femoral head as well as acetabulum |
| V | Aspherical congruency seen | Flattened femoral head with normal femoral neck and acetabulum |
| LCPD: Legg–Calve–Perthes disease | | |

| Table 3: Modified Elizabethtown classification of LCPD. | |
|---|---|
| **Stage** | **Findings on radiograph** |
| Ia | Partial/complete sclerosis of the epiphysis with no loss of height |
| Ib | Sclerosis of the epiphysis with loss of height but no fragmentation |
| IIa | Early fragmentation with just one or two vertical fissures in the epiphysis on the AP or frog leg lateral view |
| IIb | Advanced fragmentation with no new bone lateral to the fragmented epiphysis |
| IIIa | Early "porotic" new bone formation at the periphery of the necrotic epiphysis, which covers less than a third of the epiphysis |
| IIIb | New bone formation of "normal" texture and covers more than a third of the epiphysis. |
| IV | Complete healing with no radiographically identifiable avascular bone. |
| AP: Anteroposterior, LCPD: Legg–Calve–Perthes disease | |

prognosis despite the age of presentation, and Grade II disease has a better prognosis if the age of presentation is <4 years. Grades III and IV have poor prognosis [Figure 9].

Herring classification is based on the extent of involvement of the lateral pillar and carries the best reproducibility [Table 5].[22,26] The Herring classification should be applied during the fragmentation stage. According to this classification, the femoral head is divided into three parts, namely, the lateral pillar (15–30% of the lateral part of the femoral head), central pillar (central 50% of the head), and medial pillar (25–30% of the medial part of the head). The more the lateral pillar is involved, the poorer is the prognosis.

The Growth Plate Involvement (GPI) index is a product of the ratio between the affected width of the femoral head on anteroposterior and frog-leg views and carries high reproducibility.

GPI = (affected width/entire width) on anteroposterior (AP)

**Table 4:** Modified Catterall classification of LCPD.

| Stage | Extent of necrosis of femoral head |
|---|---|
| I | Minimal anterior epiphyseal involvement with no involvement of the metaphysis |
| II | Anterior epiphyseal involvement of <50% with possible involvement of metaphysis |
| III | Anterior epiphyseal involvement >50% frequently involving the metaphysis |
| IV | Total involvement of the epiphysis and metaphysis. |

LCPD: Legg–Calve–Perthes disease

**Table 5:** Herring classification of LCPD.

| Stage | Extent of involvement of lateral pillar |
|---|---|
| A | Lateral pillar uninvolved |
| B | >50% of the height of lateral pillar is preserved |
| C | Involvement of >50% of lateral pillar height |

LCPD: Legg–Calve–Perthes disease
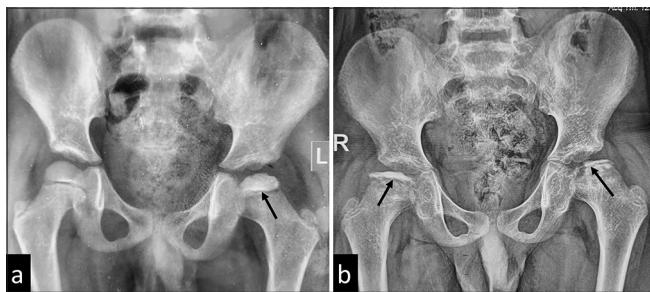


**Figure 9:** (a) Plain radiograph of a child with Catterall stage I Perthe's disease of left hip. The arrow shows minimal epiphyseal involvement. (b) Radiograph of the same child showing progression of disease over 11 months to bilateral Catterall Stage IV disease. The arrows show bilateral, total epiphyseal involvement.

view × (affected width/entire width) on frog-leg view.

- Type I – if GPI is <0.25 and is associated with Herring stage A or A/B.
- Type II – if GPI ≥0.25 and is associated with Herring stage B/C or C.

Similar features may also be demonstrated on hip ultrasonography with measurement of the hip extrusion angles, which are similar to the Graf angles for DDH. In addition, joint effusion is also best demonstrated with ultrasonography.[27-29]

### MRI

MRI plays a complementary role in addition to plain radiographs, thus increasing diagnostic confidence even in cases with equivocal radiographs. MRI also helps in early diagnosis, accurate staging of disease, identification of complications, and ruling out differentials, such as epiphyseal dysplasias, without risk of ionizing radiation.[21] The percentage of femoral head involvement can be calculated accurately on MRI with an evaluation of the bony as well as cartilaginous changes, thereby predicting the risk of collapse of the head.[21] Contrast-enhanced MRI helps in evaluation of femoral head perfusion, and the presence of enhancement is a good prognostic indicator.[30-32] Diffusion-weighted imaging has been shown to be more sensitive in picking up ischemic regions in the femoral head, even before enhancement deficits.[21,33,34]

In the early/avascular phase, MRI shows a low T1 signal of epiphysis with varying degrees of bone marrow edema. A subchondral T2 hyperintense/T1 hypointense line may be noted, known as the Crescent/Caffey's sign, indicating a subchondral fracture [Figure 10].[21] Enhancement deficits may be visualized predominantly in the anterior portion of the femoral head. In late stages, deformation, fragmentation,
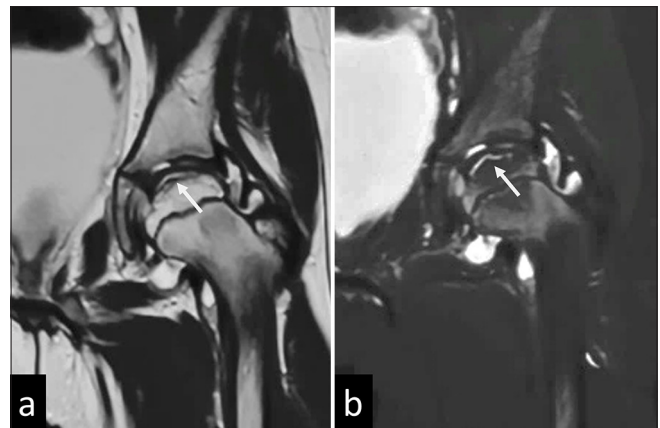


**Figure 10:** (a) T2 and (b) Short tau inversion recovery (STIR) images of magnetic resonance imaging of the left hip in a child with Perthes disease showing a T2/STIR hyperintense subchondral fracture line (white arrows) suggestive of Crescent sign/Caffey's sign.

or collapse of the femoral head may be noted with abnormal thickening of the overlying cartilage and the adjacent labrum [Figure 11].[35] Metaphyseal cystic changes may be seen with metaphyseal cupping; the presence of metaphyseal cysts is considered a poor prognosis. Associated synovitis and pannus formation may be best depicted on contrast enhanced sequences.[36]

## Management

Patient's age, Stulberg classification, and extent of lateral pillar involvement guide the management of LCPD. It has been shown that the chance of a good outcome decreases with age at onset.[37] The goal of surgery is to prevent loss of joint congruence by bringing back the epiphysis to its central position. In patients with >50% epiphyseal involvement, femoral varus osteotomy and Salter's osteotomy are associated with good outcomes. In severe LCPD, triple pelvic osteotomy or a combination of Salter's osteotomy and femoral varus osteotomy are performed.[37]

## Summary

LCPD represents idiopathic osteonecrosis of the femoral head, affecting young boys. Radiographs and MRI are the imaging modalities commonly used for the diagnosis and prognostication of LCPD. Various classification/grading systems, such as the Stulberg classification, modified Elizabethtown classification, modified Catterall classification, and modified Herring/lateral pillar classification, can be applied on radiographs to prognosticate and guide the management of LCPD. Treatment is mainly surgical and includes femoral varus osteotomy, Salter's osteotomy, and triple pelvic osteotomy.
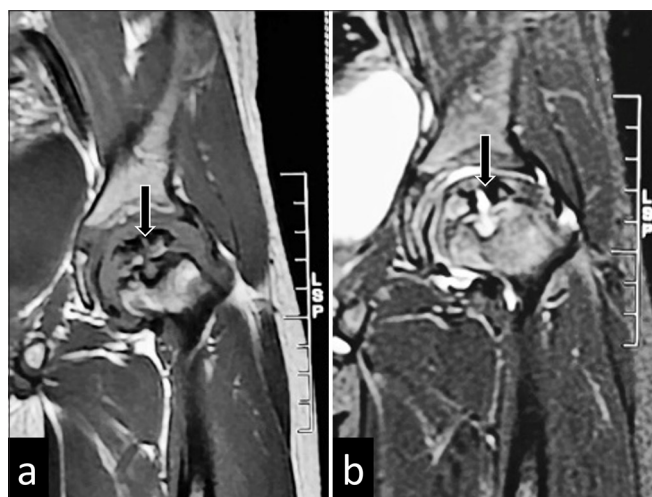


**Figure 11:** (a) T2 and (b) Short tau inversion recovery images of magnetic resonance imaging of the left hip in a child with Perthes disease showing disintegrated ossific nuclei (black arrows).

## SCFE

Also known as slipped upper femoral epiphysis, it is one of adolescents' most common hip abnormalities.[38] It commonly affects boys between 12 and 15 years of age. However, when girls are affected, the age of presentation is earlier – between 10 and 13 years of age.[39,40] SCFE may be bilateral in 18–63% of patients.[41]

### Risk factors and etiopathogenesis

Various metabolic, endocrinological, hormonal, and immunological causes of SCFE have been described.[42] Obesity in the rapid growth phase of adolescence is the most commonly associated risk factor. Rapid weight gain leads to weakening of the femoral physis and shearing stress, resulting in SCFE. Other mechanical factors include acetabular/femoral retroversion and physis inclination. Endocrinological factors include hypothyroidism, hypovitaminosis D, and chronic renal failure.[43] Chronic diseases alter the growth hormone-insulin-like growth factor – 1 axis, increasing the risk of developing SCFE.

SCFE is essentially a type I Salter Harris injury, characterized by the anterior, superior, and lateral displacement of the femoral metaphysis, corresponding to the posteromedial slip of the epiphysis. During a growth spurt, the physeal axis becomes more oblique, subjecting it to an increased risk of slippage from shear forces. The slip may be categorized as stable or unstable, depending on the ability to bear weight. Complications of SCFE include AVN of the femoral head, femoroacetabular impingement (FAI), and early osteoarthritis. The femoral capital slip injures the lateral epiphyseal arteries, affecting the vascularity of the weight-bearing surface and resulting in AVN.[44,45] FAI results from the decreased offset at the femoral head-neck junction due to the abnormal femoral head position. Cam deformity may be present even in subclinical SCFE.[46]

### Clinical presentation

SCFE is classified as "stable" or "unstable" disease, depending on the ability of the patient to bear weight (for example, while walking). The clinical presentation varies between the two types. A patient with stable SCFE presents with a vague pain localized to the hip or groin. A slight limp may be associated, and there may be external rotation of gait. There is no preceding trauma. On the other hand, a patient with unstable SCFE has severe hip pain and is unable to walk. On examination, the patient has an external rotation of the affected side and resists passive hip movements.

SCFE can also be divided into acute, acute-on-chronic, and chronic diseases based on the duration of symptoms. In acute SCFE, there is sudden epiphyseal displacement with symptoms <3 weeks. Chronic SCFE is characterized by

remissions and relapses, with a duration >3 weeks. Acute-on-chronic SCFE is diagnosed when hip pain is present for longer than 3 weeks, with acute exacerbations of pain.[47]

**Imaging in SCFE**

Radiography is the first-choice modality in suspected SCFE and is quite sensitive even for the imminent or "pre-slip" stage. Indirect signs of epiphyseal displacement may be visualized on ultrasonography. MRI is more sensitive than radiography in the pre-slip stage and can detect the complications of SCFE, such as AVN and FAI. CT can delineate the post-slip deformity and help in surgical planning.

*Radiography*

Anteroposterior and frog-leg lateral views of the pelvis and both hips should be obtained [Figure 12]. It is essential to include the contralateral hip since it serves as a control to compare with the affected side. Furthermore, due to the high incidence of bilateral involvement, the clinically normal hip should be adequately analyzed to rule out an imminent slip.[48] In an unstable slip, the frog-leg lateral view may be painful and increase the slippage. In such cases, a cross-table view in lateral decubitus is often more comfortable.

The pre-slip stage is characterized by the widening of the physeal plate with irregularity of physeal edges. The slip has not occurred yet, so the epiphysis and the femoral neck are normal at this stage.

The epiphyseal slip is predominantly posterior and, to a lesser extent, medial. On the frontal radiograph, a tangential line drawn along the superior border of the femoral neck (*Klein's line*) normally intersects the femoral epiphysis. However, in SCFE, due to the posteromedial slip of the femoral epiphysis, Klein's line does not intersect it (*Trethowan sign*). However, this sign may not be obvious in subtle cases with mild slips. In such cases, SCFE is diagnosed by asymmetry between the lines of Klein in both hips – if the width of the epiphysis lateral

to the Klein's line differs by more than 2 mm compared to the contralateral side, it indicates mild SCFE.[49] The "*metaphyseal blanch sign*" refers to the crescentic opacity projecting over the metaphysis, resulting from the superimposition of the posteriorly displaced femoral epiphysis.[50] There is an associated reduction of femoral epiphyseal height.

In cases of chronic SCFE, there may be cystic changes at the metaphysis associated with periosteal reaction. Complications of SCFE, such as AVN, present with respective findings on radiography.

*Ultrasonography*

On ultrasonography, the posterior epiphyseal displacement is visualized with a physeal step. Other associated findings include reduced distance between the anterior rim of the acetabulum and the metaphysis, remodeling of the epiphysis, and joint effusion.[51-53]
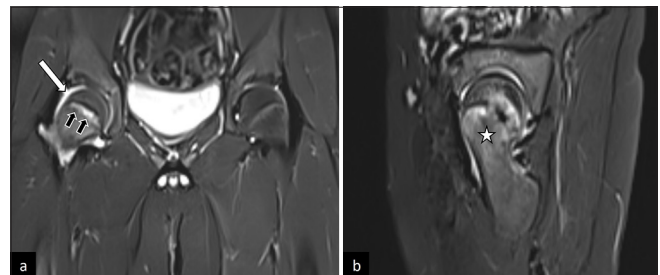
*CT*

The role of CT in the diagnosis of SCFE is limited; however, it may be useful in pre-surgical planning and in diagnosing complications in chronic SCFE.

*MRI*

MRI is particularly useful in the pre-slip stage of SCFE when the displacement of the femoral head is not seen on radiographs. In this stage, the findings on MRI include widening of the physis with marrow edema of the metaphysis, synovitis, and joint effusion [Figure 13].[48,54] Pre-existing AVN of the femoral head is best visualized and prognosticated on diffusion-weighted imaging.[55]

In established SCFE, MRI shows the epiphyseal slip with associated synovial thickening and joint effusion. Post-contrast sequences are helpful to look for synovitis and rule out AVN [Figure 14].



**Figure 12:** (a) Frontal and (b) frog-leg lateral views in a child with slipped capital femoral epiphysis highlighting the importance of frog leg lateral view-the frontal radiograph shows that only subtle disparity is seen in epiphyseal heights (reduced height on left side), whereas the slip better appreciated in the frog leg lateral radiograph.



**Figure 13:** (a) Coronal, and (b) sagittal T2-weighted images in a patient with pre-slip stage of right sided slipped capital femoral epiphysis. There is widening of the physis (black arrows in a), with synovitis and joint effusion (white arrow in a) and marrow edema of the metaphysis (white asterik in b). This patient had a complete slip on follow-up imaging.
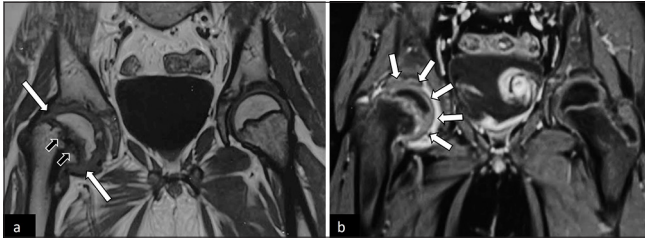
**Figure 14:** (a) Coronal T1-weighted and (b) post-contrast magnetic resonance images of pelvis with both hip joints in an adolescent with the right-sided limp, showing slipped right capital femoral epiphysis (white arrows in a) with periphyseal bone marrow edema (black arrows in a). There was associated synovitis (white arrows in b) with no suggestion of avascular necrosis.

FAI is an important complication of SCFE and can lead to cartilage loss, most commonly in the anterior/superior quadrant.[56] Labral hypertrophy and degeneration have also been observed. Cartilage injury is characterized by thinning and fissuring on conventional magnetic resonance sequences. Dedicated sequences for cartilage imaging such as delayed Gadolinium-enhanced MRI of cartilage, T1rho imaging and gag chemical exchange saturation transfer are more sensitive.[57]

**Imaging considerations in treatment**

The severity of SCFE on radiographs is represented by the degree of femoral head displacement, graded by the Southwick angle and posterior sloping angle. The *Southwick angle* is measured on the frog-leg lateral view [Figure 15]. A line is drawn along the axis of the femoral shaft. Another line is drawn perpendicular to a line connecting the anterior and posterior margins of the physis. The angle between these two lines is the Southwick angle ($\alpha$). This angle usually is 12° and increases in SCFE. For quantifying the posterior head-neck angulation, the Southwick angle of the normal hip is subtracted from that of the hip with SCFE. The severity is then graded as mild (0–30°), moderate (30°–50°), and severe (>50°).[58]

The *posterior sloping angle* is used to assess the bilaterality of SCFE. Similar to the Southwick angle, two lines are drawn on the frog-leg lateral view, one connecting the ends of femoral physis, and the other along the femoral shaft axis. Then, a line is drawn perpendicular to the axis of the femoral shaft, and the angle between this line and the physeal line is the posterior sloping angle [Figure 16]. Values of 12°–15° are predictive of contralateral SCFE and necessitate prophylactic pinning.[59] The posterior sloping angle has a significant correlation with the time to development of contralateral SCFE and is the only independent risk factor for the same.[60,61]



**Figure 15:** Southwick angle. On the frog-leg lateral view, a line is drawn along the axis of the femoral shaft. Another line (dotted) is drawn perpendicular to a line connecting the anterior and posterior margins of the physis. The angle between these two lines is the Southwick angle (alpha).



**Figure 16:** Posterior sloping angle. Two lines are drawn on frog-leg lateral view, one connecting the ends of femoral physis and the other along the femoral shaft axis. Then, a line is drawn perpendicular to the axis of the femoral shaft (dotted line) and the angle between this line and the physeal line is the posterior sloping angle.

**Management**

The severity and stability of SCFE are essential factors in deciding surgical management. Stable SCFE with mild-to-moderate slips are pinned *in situ*. Stable SCFE with severe slips and unstable SCFE with any degree of slip is

first reduced and are followed up with pin or wire fixation. Stable SCFE with severe slip may also require an osteotomy to improve femoral head alignment and prevent early osteoarthritis.[62]

**Summary**

SCFE, a type I Salter Harris injury of the femoral epiphysis, affects adolescent boys. Radiography is the first investigation in suspected SCFE. Indirect signs of epiphyseal displacement may be visualized on ultrasonography. MRI is more sensitive than radiography in the pre-slip stage and can detect the complications of SCFE, such as AVN and FAI. CT helps in surgical planning. The Southwick angle and posterior sloping angle are used to assess the severity of SCFE on radiographs. The management depends on the stability and severity of SCFE.

## CONCLUSION

DDH, LCPD, and SCFE constitute the common developmental disorders of the hip joint in the pediatric and adolescent population. A high clinical suspicion is required to narrow down the differential diagnosis and choose the appropriate imaging modality. Imaging plays a key role in the timely diagnosis of these conditions and guides in the appropriate management. Each modality has its strengths and limitations, and a tailored approach often provides the most comprehensive assessment. US is the primary imaging modality in neonates/infants with DDH, before ossification. Radiographs are commonly used in all three disorders as a first-line investigation and in follow-up. MRI plays a complementary role and provides excellent soft-tissue characterization. It is, thus, essential for the radiologist to be aware of the preferred imaging modality and the common imaging findings in these conditions.

## REFERENCES

1. Lee MC, Eberson CP. Growth and development of the child's hip. Orthop Clin North Am 2006;37:119-32.
2. Strayer LM Jr. Embryology of he human hip joint. Clin Orthop Relat Res 1971;74:221-40.
3. Harrison TJ. The influence of the femoral head on pelvic growth and acetabular form in the rat. J Anat 1961;95:12-24.
4. Lehmann HP, Hinton R, Morello P, Santoli J. Developmental dysplasia of the hip practice guideline: Technical report. Committee on quality improvement, and subcommittee on developmental dysplasia of the hip. Pediatrics 2000;105:E57.
5. Nandhagopal T, Tiwari V, De Cicco FL. Developmental dysplasia of the hip. In: StatPearls. Treasure Island, FL: StatPearls Publishing; 2024. Available from: https://www.ncbi.nlm.nih.gov/books/NBK563157 [Last accessed on 2024 Oct 21].
6. Bakarman K, Alsiddiky AM, Zamzam M, Alzain KO, Alhuzaimi FS, Rafiq Z. Developmental dysplasia of the hip (DDH): Etiology, diagnosis, and management. Cureus 2023;15:e43207.
7. Sarban S, Ozturk A, Tabur H, Isikan UE. Anteversion of the acetabulum and femoral neck in early walking age patients with developmental dysplasia of the hip. J Pediatr Orthop B 2005;14:410-4.
8. Wang W, Zhuang W, Zeng W, Feng Y, Zhang Z. Review of susceptibility genes in developmental dysplasia of the hip: A comprehensive examination of candidate genes and pathways. Clin Genet. 2025;107:3-12.
9. Feldman G, Kappes D, Mookerjee-Basu J, Freeman T, Fertala A, Parvizi J. Novel mutation in Teneurin 3 found to co-segregate in all affecteds in a multi-generation family with developmental dysplasia of the hip. J Orthop Res 2019;37:171-80.
10. Feldman G, Dalsey C, Fertala K, Azimi D, Fortina P, Devoto M, *et al.* The Otto Aufranc award: Identification of a 4 Mb region on chromosome 17q21 linked to developmental dysplasia of the hip in one 18-member, multigeneration family. Clin Orthop Relat Res 2010;468:337-44.
11. Noordin S, Umer M, Hafeez K, Nawaz H. Developmental dysplasia of the hip. Orthop Rev (Pavia) 2010;2:e19.
12. French LM, Dietz FR. Screening for developmental dysplasia of the hip. Am Fam Physician 1999;60:177-84, 187-8.
13. Starr V, Ha BY. Imaging update on developmental dysplasia of the hip with the role of MRI. Am J Roentgenol 2014;203:1324-35.
14. Karnik A, Lawande A, Lawande MA, Patkar D, Aroojis A, Bhatnagar N. Practice essentials of imaging in early diagnosis of DDH. Indian J Orthop 2021;55:1466.
15. Aroojis A, Anne RP, Li J, Schaeffer E, Kesavan TM, Shah S, *et al.* Surveillance for developmental dysplasia of the hip in India: Consensus guidelines from the pediatric orthopaedic society of India, Indian academy of pediatrics, national neonatology forum of India, Indian radiological and imaging association, Indian federation of ultrasound in medicine and biology, federation of obstetric and gynaecological societies of India, and Indian orthopaedic association. Indian Pediatr 2022;59:626-35.
16. Ghasseminia S, Hareendranathan AR, Jaremko JL. Narrative review on the role of imaging in DDH. Indian J Orthop 2021;55:1456-65.
17. AIUM practice parameter for the performance of the ultrasound examination for detection and assessment of developmental dysplasia of the hip. J Ultrasound Med 2024;43:E33-8.
18. Graf R, Scott S, Lercher K, Baumgartner F, Benaroya A.

Hip sonography: Diagnosis and management of infant hip dysplasia. In: Hip sonography: Diagnosis and management of infant hip dysplasia. Berlin: Springer; 2006. p. 1-114.

19. Weinstein SL, Mubarak SJ, Wenger DR. Fundamental concepts of developmental dysplasia of the hip. Instr Course Lect 2014;63:299-305.

20. Vaquero-Picado A, González-Morán G, Garay EG, Moraleda L. Developmental dysplasia of the hip: Update of management. EFORT Open Rev 2019;4:548-56.

21. Dillman JR, Hernandez RJ. MRI of Legg-Calvé-Perthes disease. AJR Am J Roentgenol 2009;193:1394-407.

22. Rampal V, Clément JL, Solla F. Legg-Calvé-Perthes disease: Classifications and prognostic factors. Clin Cases Miner Bone Metab 2017;14:74-82.

23. Podeszwa DA, DeLaRocha A. Clinical and radiographic analysis of Perthes deformity in the adolescent and young adult. J Pediatr Orthop 2013;33 Suppl 1:S56-61.

24. Joseph B, Varghese G, Mulpuri K, Rao KL, Nair NS. Natural evolution of Perthes disease: A study of 610 children under 12 years of age at disease onset. J Pediatr Orthop 2003;23:590-600.

25. Christensen F, Søballe K, Ejsted R, Luxhøj T. The Catterall classification of Perthes' disease: An assessment of reliability. J Bone Joint Surg Br 1986;68:614-5.

26. Herring JA, Kim HT, Browne R. Legg-Calve-Perthes disease. Part I: Classification of radiographs with use of the modified lateral pillar and Stulberg classifications. J Bone Joint Surg Am 2004;86:2103-20.

27. Jandl NM, Schmidt T, Schulz M, Rüther W, Stuecker MH. MRI and sonography in Legg-Calvé-Perthes disease: Clinical relevance of containment and influence on treatment. J Child Orthop 2018;12:472-9.

28. Wirth T, LeQuesne GW, Paterson DC. Ultrasonography in Legg-Calvé-Perthes disease. Pediatr Radiol 1992;22:498-504.

29. Naumann T, Kollmannsberger A, Fischer M, Puhl W. Ultrasonographic evaluation of Legg-Calve-Perthes disease based on sonoanatomic criteria and the application of new measuring techniques. Eur J Radiol 1992;15:101-6.

30. Lamer S, Dorgeret S, Khairouni A, Mazda K, Brillet PY, Bacheville E, *et al.* Femoral head vascularisation in Legg-Calvé-Perthes disease: Comparison of dynamic gadolinium-enhanced subtraction MRI with bone scintigraphy. Pediatr Radiol 2002;32:580-5.

31. Sebag G, Ducou Le Pointe H, Klein I, Maiza D, Mazda K, Bensahel H, *et al.* Dynamic gadolinium-enhanced subtraction MR imaging--a simple technique for the early diagnosis of Legg-Calvé-Perthes disease: Preliminary results. Pediatr Radiol 1997;27:216-20.

32. Uno A, Hattori T, Noritake K, Suda H. Legg-Calvé-Perthes disease in the evolutionary period: Comparison of magnetic resonance imaging with bone scintigraphy. J Pediatr Orthop 1995;15:362-7.

33. Gracia G, Baunin C, Vial J, Accadbled F, Sales de Gauzy J. Diffusion-weighted MRI for outcome prediction in early Legg-Calvé-Perthes disease: Medium-term radiographic correlations. Orthop Traumatol Surg Res 2019;105:547-50.

34. Baunin C, Sanmartin-Viron D, Accadbled F, Sans N, Vial J, Labarre D, *et al.* Prognosis value of early diffusion MRI in Legg Perthes Calvé disease. Orthop Traumatol Surg Res 2014;100:317-21.

35. Jaramillo D, Kasser JR, Villegas-Medina OL, Gaary E, Zurakowski D. Cartilaginous abnormalities and growth disturbances in Legg-Calvé-Perthes disease: Evaluation with MR imaging. Radiology 1995;197:767-73.

36. Rush BH, Bramson RT, Ogden JA. Legg-Calvé-Perthes disease: Detection of cartilaginous and synovial change with MR imaging. Radiology 1988;167:473-6.

37. Leroux J, Abu Amara S, Lechevallier J. Legg-Calvé-Perthes disease. Orthop Traumatol Surg Res 2018;104:S107-12.

38. Lehmann CL, Arons RR, Loder RT, Vitale MG. The epidemiology of slipped capital femoral epiphysis: An update. J Pediatr Orthop 2006;26:286-90.

39. Kaneetah AH, Alosaimi MN, Ismail AA, Alansari AO. Unusual age of presentation and etiology of slipped capital femoral epiphysis following a seizure attack: A case report. Cureus 2022;14:e30772.

40. Miles DT, Wilson AW, Scull MS, Moses W, Quigley RS. A new look on the epidemiology of slipped capital femoral epiphysis: A topic revisited. J Pediatr Orthop Soc North Am 2023;5:705.

41. Loder RT, Aronsson DD, Weinstein SL, Breur GJ, Ganz R, Leunig M. Slipped capital femoral epiphysis. Instr Course Lect 2008;57:473-98.

42. Pritchett JW, Perdue KD. Mechanical factors in slipped capital femoral epiphysis. J Pediatr Orthop 1988;8:385-8.

43. Witbreuk M, van Kemenade FJ, van der Sluijs JA, Jansma EP, Rotteveel J, van Royen BJ. Slipped capital femoral epiphysis and its association with endocrine, metabolic and chronic diseases: A systematic review of the literature. J Child Orthop 2013;7:213-23.

44. Brodetti A. The blood supply of the femoral neck and head in relation to the damaging effects of nails and screws. J Bone Joint Surg Br Vol 1960;42-B:794-801.

45. Jarrett D, Matheney T, Kleinman P. Imaging SCFE: Diagnosis, treatment and complications. Pediatr Radiol 2013;43 Suppl 1:S71-82.

46. Fraitzl CR, Käfer W, Nelitz M, Reichel H. Radiological evidence of femoroacetabular impingement in mild slipped capital femoral epiphysis: A mean follow-up of 14.4 years after pinning *in situ*. J Bone Joint Surg Br 2007;89:1592-6.

47. Aprato A, Conti A, Bertolo F, Massè A. Slipped capital femoral epiphysis: Current management strategies. Orthop Res Rev 2019;11:47-54.

48. Hesper T, Zilkens C, Bittersohl B, Krauspe R. Imaging modalities in patients with slipped capital femoral epiphysis. J Child Orthop 2017;11:99-106.

49. Green DW, Mogekwu N, Scher DM, Handler S, Chalmers P, Widmann RF. A modification of Klein's Line to improve sensitivity of the anterior-posterior radiograph in slipped capital femoral epiphysis. J Pediatr Orthop 2009;29:449-53.

50. Steel HH. The metaphyseal blanch sign of slipped capital femoral epiphysis. J Bone Joint Surg Am 1986;68:920-2.

51. Palaniappan M, Indiran V, Maduraimuthu P. Ultrasonographic diagnosis of slipped capital femoral epiphysis. Polish J Radiol 2017;82:149.

52. Kallio PE, Lequesne GW, Paterson DC, Foster BK, Jones JR. Ultrasonography in slipped capital femoral epiphysis. Diagnosis and assessment of severity. J Bone Joint Surg Br 1991;73:884-9.

53. Terjesen T. Ultrasonography for diagnosis of slipped capital femoral epiphysis: Comparison with radiography in 9 cases. Acta Orthop Scand 1992;63:653-7.

54. Lalaji A, Umans H, Schneider R, Mintz D, Liebling MS, Haramati N. MRI features of confirmed "pre-slip" capital femoral epiphysis: A report of two cases. Skelet Radiol 2002;31:362-5.

55. Mueller D, Schaeffeler C, Baum T, Walter F, Rechl H, Rummeny EJ, *et al.* Magnetic resonance perfusion and diffusion imaging characteristics of transient bone marrow edema, avascular necrosis and subchondral insufficiency fractures of the proximal femur. Eur J Radiol 2014;83:1862-9.

56. Sink EL, Zaltz I, Heare T, Dayton M. Acetabular cartilage and labral damage observed during surgical hip dislocation for stable slipped capital femoral epiphysis. J Pediatr Orthop 2010;30:26-30.

57. Zilkens C, Miese F, Bittersohl B, Jäger M, Schultz J, Holstein A, *et al.* Delayed gadolinium-enhanced magnetic resonance imaging of cartilage (dGEMRIC), after slipped capital femoral epiphysis. Eur J Radiol 2011;79:400-6.

58. Loder RT, Aronsson DD, Dobbs MB, Weinstein SL. Slipped capital femoral epiphysis. Instr Course Lect 2001;50:555-70.

59. Barrios C, Blasco MA, Blasco MC, Gascó J. Posterior sloping angle of the capital femoral physics: A predictor of bilaterality in slipped capital femoral epiphysis. J Pediatr Orthop 2005;25:445-9.

60. Boyle MJ, Lirola JF, Hogue GD, Yen YM, Millis MB, Kim YJ. The alpha angle as a predictor of contralateral slipped capital femoral epiphysis. J Child Orthop 2016;10:201-7.

61. Nötzli HP, Wyss TF, Stoecklin CH, Schmid MR, Treiber K, Hodler J. The contour of the femoral head-neck junction as a predictor for the risk of anterior impingement. J Bone Joint Surg Br 2002;84:556-60.

62. Parsch K, Weller S, Parsch D. Open reduction and smooth Kirschner wire fixation for unstable slipped capital femoral epiphysis. J Pediatr Orthop 2009;29:1-8.